The Five Twin Laws of Gypsum (CaSO4 center dot 2H(2)O): A Theoretical Comparison of the Interfaces of the Contact Twins

ARTICLE *in* CRYSTAL GROWTH & DESIGN · JANUARY 2012

Impact Factor: 4.89 · DOI: 10.1021/cg201031s

4 AUTHORS:

Marco Rubbo
Università degli Studi di Torino
98 PUBLICATIONS **614** CITATIONS
SEE PROFILE

Marco Bruno
Università degli Studi di Torino
84 PUBLICATIONS **706** CITATIONS
SEE PROFILE

Francesco Roberto Massaro
University of Padova
41 PUBLICATIONS **286** CITATIONS
SEE PROFILE

Dino Aquilano
Università degli Studi di Torino
190 PUBLICATIONS **998** CITATIONS
SEE PROFILE

CRYSTAL GROWTH & DESIGN

Article

pubs.acs.org/crystal

The Five Twin Laws of Gypsum ($CaSO_4 \cdot 2H_2O$): A Theoretical Comparison of the Interfaces of the Contact Twins

Marco Rubbo,*[,†] Marco Bruno,[†] Francesco Roberto Massaro,[‡] and Dino Aquilano[†]

[†]Dipartimento di Scienze Mineralogiche e Petrologiche, Università degli Studi di Torino, via V. Caluso 35, I-10125 Torino, Italy

[‡]Dipartimento di Scienza dei Materiali, Università di Milano Bicocca, via R. Cozzi 53, I-20125 Milano, Italy

Supporting Information

ABSTRACT: The relaxed interfaces of the 100, $\bar{1}01$, 001, $20\bar{1}$, and 101 contact twins of the gypsum crystal are theoretically examined, and their perturbed structure is described. The obtained twin energies (γ_{PT}) are 13.6, 145, 255, 826, and 848 erg cm^{-2} for the 100, 001, $\bar{1}01$, $20\bar{1}$, and 101 laws, respectively. Hence, the five twin laws can be divided in three classes reflecting the deep difference due to the character of the face, in the sense of Hartman−Perdok, on which the contact twin is supposed to form. In fact, the original composition planes of the 100, 001, and $\bar{1}01$ laws correspond to stepped (S) faces, while those of the $20\bar{1}$ and 101 laws correspond to kinked (K) faces. Furthermore, the highest probability of occurrence of the 100 contact twins is strictly related not only to the lowest γ_{PT} value but also to the fact that, among the three S faces, (100) is the only one belonging to the athermal equilibrium shape of the crystal.

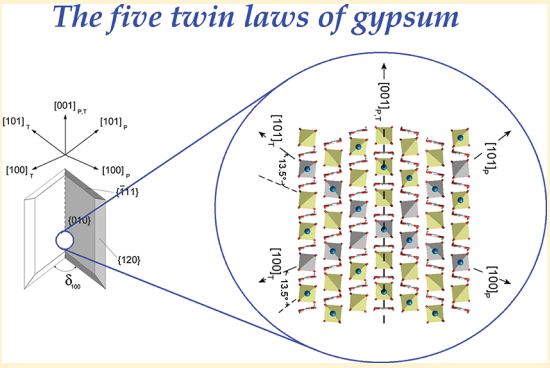

1. INTRODUCTION

In recent papers, the theoretical and athermal (T = 0 K) equilibrium morphology of gypsum was evaluated,[1] and a theoretical analysis was performed on the development of the stepped prisms belonging to the main [001] zone. The conclusions were strengthened by the agreement between the predicted equilibrium morphology of the [001] zone and that of the giant crystals of Naica mine,[2] which grew very close to the thermodynamic equilibrium.[3] Recently, the theoretical structure of the 100 contact twin was investigated, and the athermal twinning and adhesion energies were determined by minimizing the twin energy.[4]

Here, we report on the continuation of this systematic study on the theoretical equilibrium and growth morphology of gypsum. Indeed, a deeper knowledge of twinning (either contact or penetration) is required. Five laws[5] describe gypsum twins, but as far as we know, no studies have dealt with the structures of the interfaces, and very few on the energies have involved their generation. As a matter of fact, the "geometry of the twins" awakened great interest since the times of Romé de l'Isle and Haüy and was described and set systematically in the papers by Mallard[6] and Friedel,[7] and the genetic mechanisms of the "growth twins" has been thoroughly treated, for the first time, as late as at the end of the 1950s, by Curien and Kern.[8]

In this paper, starting from these works, we will attempt to determine a theoretical hierarchy among the five twin laws of gypsum, confining our attention to the contact twins, and we will compare the calculated twin energies with their probability of occurrence obtained from the literature data about natural and artificial crystals. In a forthcoming paper, we will deal with the homologous penetration twins, assuming the 010 plane as the original composition plane (OCP),[8] to compare, for each twin law, the probability of nucleation of a given twin, either by contact or by penetration.

The reader is referred to the well-documented papers by Cody and Cody[9,10] on the observed occurrence frequency of gypsum twins, where over six decades of gypsum literature are summarized. It is a merit of this paper to give reasons to be critical on the proposed identifications of the most frequently occurring twin laws.

As throughout more than two centuries of investigations on the morphology of gypsum twins a variety of reference frames were adopted, we put at the reader's disposal the relationships among them in the Appendix. This is certainly not due to an excess of zeal but simply to the fact that people working on crystal morphology and those determining crystal structure often find difficulty in communicating each other.

2. THE CHOICE OF THE REFERENCE FRAME

We adopted in this paper the reference frame chosen by De Jong and Bouman,[11] Cole and Lancucki,[12] and Hejinen and Hartman[13] (see Table 1). Our choice was grounded on two main reasons:

– This frame uses the smallest and the second smallest vectors of the four possible lattice vectors.

Received: August 9, 2011
Revised: November 15, 2011
Published: November 21, 2011

Table 1. Cell Parameters (Å) and Related Space Groups Referred to the Morphological Cell by Friedel[14] (0.372:1:0.412; β = 113.83°)

a_0	b_0	c_0	β (°)	space group	authors
5.63	15.15	6.23	113.83	$C2/c$	De Jong and Bouman[11]
5.67	15.201	6.274	113.91	$A2/a$	Cole and Lancucki[12]
5.678	15.213	6.286	114.08	$A2/a$	Hejinen and Hartman[13]

– The axis coincides with the morphological elongation of the crystals growing from pure aqueous solution and of the major part of natural crystals.

3. GEOMETRICAL DESCRIPTION OF THE FIVE TWIN LAWS

In Table 2, the data concerning the geometrical identity of the five twin laws are collected. In the first row, the indexing refers to the mirror planes that relate the reference frames of the parent (P) and twinned (T) crystals. With T, we indicate the crystal generated from P by the twin operations.

In the second one, the twinning operation is described by the A_2 axis lying in the twin plane and perpendicular to the [010] diad axis: this is an important structural feature, that is, the row parallel to the A_2 axis is common to both P and T individuals. It is worth remembering that the operations described in the first and second row are equivalent. Actually, in gypsum, a *h*0*l* mirror plane does not change the direction of the [010] diad axis, while any A_2 axis coincident with a [*u*0*w*] direction changes the [010] direction in the [0$\bar{1}$0] one; nevertheless, [010] and [0$\bar{1}$0] directions are equivalent in gypsum crystal because of the 010 glide symmetry plane.

The third row shows the areas of the 2D coincidence meshes at the P/T interfaces. The meshes are nearly rectangular, defined by the lattice vectors parallel to the twin axes and by [010], which is obviously common to all of the gypsum twins. Rows from 4 to 7 identify, for each twin law, the multiple 2D cells that can be obtained from the superposition of the P and T lattices onto their common 010 plane. In other words, following Simon,[15] we attempted to find if superlattices exist, defined by lattice points that are common to both P and T individuals.

In the fourth row are shown the vectors defining the 2D mesh on the common 010 plane of each twin:

– Items (i) and (ii) refer to the quasi-perfect multiple cells (either monoclinic or orthorhombic), that is, to those cells where the angular misfit between the lattices of P and T crystals are close to nil, as illustrated in Figure 1a,b and in the fifth row of Table 2.

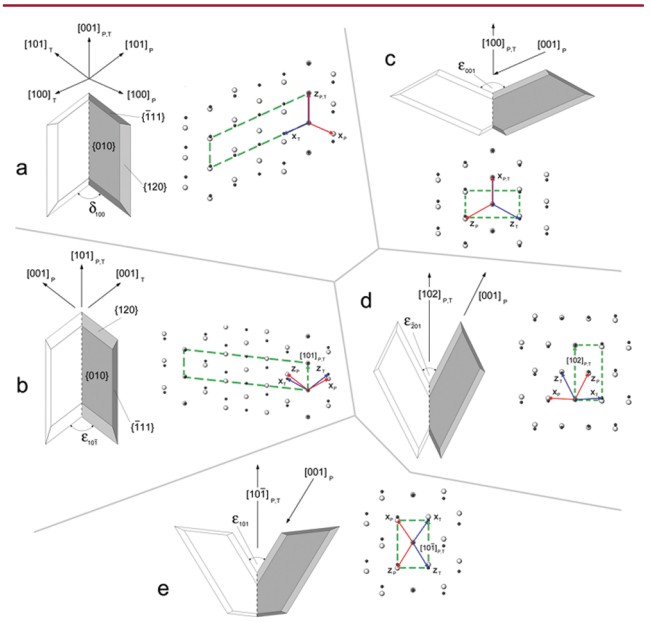

Figure 1. Geometry of the contact twins of gypsum viewed along the [010] direction. Twin laws: 100 (a), $\bar{1}$01 (b), 001 (c), 20$\bar{1}$ (d), and 101 (e). For each twin law, the contact twins have been drawn starting from the assumption that the growth rate of both {120} and {$\bar{1}$11} prisms is lower than that of the {010} pinacoid. Contact planes are represented by dashed lines. P and T stand for parent and twinned individuals, respectively. Next to each twin morphology, the corresponding 2D coincidence lattice on the common 010 plane is represented. The common 2D mesh of the coincidence lattice is also drawn. It is worth nothing that $\delta_{100} = \varepsilon_{\bar{1}01} = 105.02°$.

– Item (iii) refers to the multiple cells (pseudocells) where the angular misfit between the lattices of P and T is significant.

Table 2. Geometrical Description and Growth Aspect of the Five Twin Laws of Gypsum[a]

(1) twin plane	100 "swallow tail" or "butterfly"	$\bar{1}$01 "Montmartre" or "spear head" or "fer de lance"	001	20$\bar{1}$	101
(2) equivalent twin A_2 axis	[001]	[101]	[100]	[102]	[10$\bar{1}$]
(3) area of the common 2D mesh (Å^2) at the interface of the contact twin	[001] × [010] = 95.371	[101] × [010] = 99.303	[100] × [010] = 86.189	[102] × [010] = 174.599	[10$\bar{1}$] × [010] = 151.95
(4) vectors of the 2D mesh on the 010 common plane	(i) monoclinic [401] × [001]	(i) monoclinic [40$\bar{2}$] × [101]			
	(ii) orthorhombic [803] × [001]	(ii) orthorhombic [$\bar{7}$05] × [101]	(iii) pseudo-orthorhombic [100] × [102]	(iii) pseudo-orthorhombic [100] × [102]	(iii) pseudo-orthorhombic [10$\bar{1}$] × [101]
	(iii) pseudo-orthorhombic [301] × [001]	(iii) pseudo-orthorhombic [30$\bar{2}$] × [101]			
(5) 2D mesh angular misfit (°)	1.18 (i), 0.60 (ii), 2.30 (iii)	0.176 (i), 0.089 (ii), 1.19 (iii)	(iii) 2.92	(iii) 2.92	(iii) 12.81
(6) area of the 2D mesh (Å^2) on the common 010 plane	(i) = 130.08	(i) = 195.05			
	(ii) = 260.16	(ii) = 390.10	(iii) 65.04	(iii) 65.04	(iii) 65.097
	(iii) = 97.56	(iii) = 162.58			
(7) index of the twin	4 (i), 8 (ii), 3 (iii)	6 (i), 12 (ii), 5 (iii)	(iii) 2	(iii) 2	(iii) 2

[a]Both areas of the common 2D mesh and related obliquities were calculated on the basis of the Cole and Lancucki cell.[12]

dx.doi.org/10.1021/cg201031s | *Cryst. Growth Des.* 2012, 12, 264–270

In the sixth row are listed the areas of the multiple 2D cells on the common 010 plane; finally, in the seventh row, the corresponding multiplicities are given.

Some preliminary conclusions can be drawn from the geometrical data reported in Table 2. From the third row, one can see that three out of the five laws (100, $\bar{1}01$, and 001) imply 2D coincidence mesh areas very close each other (mean value, 93.62 Å^2), while the areas associated to the two remaining laws ($20\bar{1}$ and 101) are, respectively, 1.86 and 1.62 times larger than the mean value. This geometric feature is not a chance, but it has a counterpart in terms of twin energy, as we will see later.

The fourth and fifth rows indicate that quasi-perfect 2D supercells cannot be found (on the common 010 plane) in the case of 001, $20\bar{1}$, and 101 twin laws. This is an indication that embryos twinned following the 100 and $\bar{1}01$ twin laws can nucleate on the {010} faces, OCP of penetration twins,[8,15] while in the case of 001, $20\bar{1}$ and 101 twin laws, the nucleation on the {010} faces, is contrasted by a supplementary activation energy barrier, because of the elastic strain due to the angular misfit between P and T lattices. Summarizing the geometrical constraints, we can reasonably divide the five twin laws as follows:

- Contact and penetration twins following both 100 and $\bar{1}01$ laws can likely occur; furthermore, the $\bar{1}01$ penetration twins seem to be favored with respect to the 100 ones. Obviously, one cannot predict the frequency on the sole geometric considerations.
- Contact twins described by $20\bar{1}$ and 101 laws seem to be highly disadvantaged when compared to 100 and $\bar{1}01$.
- The behavior of the 001 law twins is midway between the just mentioned groups.

The considerations just drawn from Table 2 originate from the correlation between the probability of formation of an epitaxy and the multiplicity of the common 2D cell at the epitaxial interface; that is, the lower are the 2D cell area and the related parametric and angular misfit, the higher the probability of epitaxy to occur. As twinning can be considered a special epitaxy between two crystals of the same species,[16] we highlighted the relationship between the lattice twin geometry, the interfacial twin energy, and the occurrence frequency of the corresponding twin law.

In the Supporting Information, we reported the observed occurrence of twins, classified according to the five twin laws. Here, we confine our attention to focus on some structural features of the twin planes. It is interesting to remark that all of the twin planes are of the *h0l* type; that is, they belong to the [010] crystal zone, which is not an important one from the morphology point of view. As a matter of fact:

- The [010] direction does not correspond to a periodic bond chain (PBC hereinafter), in the sense of Hartman–Perdok.[17]
- None of the twin planes corresponds to a flat (F) face.
- The {100} form, which could be an OCP for the contact 100 twin, in the sense of Curien and Kern,[8] has been proven to belong to the athermal equilibrium shape (ES) of the crystal, even if it is a S face.[1]
- Both {$\bar{1}01$} and {001} forms represent other potential OCPs, for $\bar{1}01$ and 001 contact twins, respectively. As we will show later, they can belong to the ES of the crystal, even if they are stepped forms and their surface energies ($\gamma_{10\bar{1}}$ = 1010 and γ_{001} = 825 erg cm^{-2}) are much larger than those of the {100} form (γ_{100}= 616 erg cm^{-2}).
- The equivalent twin axes, respectively, [001] and [101] (i.e., the common rows of the two individuals), are PBCs of the crystals, [001] being the most important one. This means that, in principle, twinned rows can form on these faces by 1D nucleation and develop 100 and $\bar{1}01$ twinned embryos. We note that 100 and $\bar{1}01$ are the most frequently occurring twin laws.

4. THE SURFACES CORRESPONDING TO THE FIVE TWIN LAWS OF GYPSUM

When building a twinned crystal, we must comply with the symmetry, stoichiometric, and local neutrality constraints. We start from the point of view that atomic deposition during growth progressively fills layers $d_{nh,nk,nl}$ thick. The supersaturation of the mother phase plays an important role in this process determining the extent of lateral interactions between particles of the partially filled layer. We may expect that when the crystallization affinity is high, such an extended bond network can be frozen in a state not corresponding to an absolute minimum of the surface energy but nevertheless being locally neutral, stoichiometric, and satisfying the symmetry that we just observed in a twin. These configurations could be also accessed by a mechanical strain experienced by the crystal.

In kinetic terms, we can say that if a face (potentially OCP) can exist during growth at high crystallization affinity, that is, in a configuration having energy higher than the stable surface face, during the lifetime of this state, a 2D twinned nucleus may stick on the face and freeze the instantaneous configuration. Therefore, a necessary, although not sufficient, condition fulfilled by an OCP is that the corresponding stable face has a surface energy not too high.

In the Supporting Information, a detailed analysis of the character of the surfaces of gypsum is performed. Here, we only report the classification of the surfaces according to Hartman–Perdok: the (100), ($10\bar{1}$), and (001) faces have a S (stepped) character, whereas the ($20\bar{1}$) and (101) faces have a K (kinked) character.

5. THE STRUCTURES OF THE CONTACT TWIN INTERFACES AND THEIR CALCULATED TWIN ENERGIES

In the following, we describe how the contact twins are generated, and then, we characterize them. At first, a crystal slab limited by the composition plane *h0l* is reflected about a mirror plane parallel to *h0l*. To set an initial configuration of the interface between the two crystals, the original and the reflected slabs are moved one relatively to the other; ions and molecules can also be displaced to avoid evident repulsions. In this way, several initial configurations can be tested. The energy of the bicrystal is then minimized under the constraint of constant volume. Two-dimensional periodic boundary conditions are imposed repeating, in direction parallel to *h0l*, the smallest 2D cell common to both crystals. We did not define supercells because the parametric coincidence of the 2D lattices and the small translations required to obtain the structural continuity of the PBC network through the interface between one crystal and its reflected image. By the way, to afford calculations based on supercells was too heavy.

We used the program GDIS[18] to build the slabs and the program GULP[19] for the energy calculations. As in our previous works on gypsum 100 contact twin,[4] we used the force field proposed by Adam.[20] At variance with our previous works, we needed a lower tolerance on the values of the energy (*ftol* < 10^{-6}) and gradient (*gtol* < 10^{-5}) for optimization; this allowed us to obtain a mirror symmetry of the mean displacements of the plane of atoms at the interface between the P and the T crystals but only in the case of the twins having lower energy.

dx.doi.org/10.1021/cg201031s | Cryst. Growth Des. 2012, 12, 264–270

The energy of the interface is the difference of energy, per unit surface area (S), between the twinned crystal (E_{PT}) and the not twinned one ($E_{untwinned}$) comprising the same number of atoms and exhibiting the same outmost layers. Then, the twin energy is an interfacial energy (γ_{PT}) [in relation 1 of ref 4, ($E_b - E_{bw}$) must be changed in ($E_{bw} - E_b$)]:

$$\gamma_{PT} = \frac{E_{PT} - E_{untwinned}}{S} \quad (1)$$

5.1. The 100 Contact Twin. This contact twin has been extensively treated in a recently published investigation.[4] Nevertheless, its relaxed interface is illustrated is Figure 2, for the sake of comparison with the other four twins. Here, we would like to just recollect that the transition from P to T individuals is quite soft.

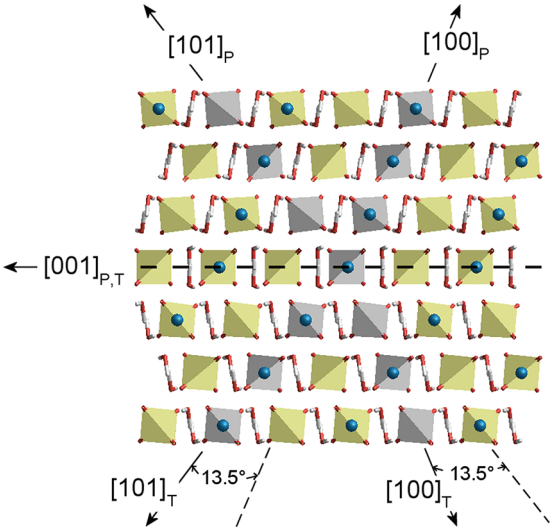

Figure 2. Contact 100 twin of gypsum after relaxation and viewed along the [010] direction. The continuity of the structure is clearly shown by the arrangement of the SO_4 tetrahedra across the twin interface, while the water molecules are strongly rearranged at the interface level. The gray color outlines the sequences building the PBCs, while the dashed lines represent their continuation in the twinned individual (see also Figure 3).

Indeed, the [100] PBCs running in the P crystal crossing the contact interface deviate by ~14° and "continue" in the [101] PBCs of the T individual. In a similar way, the [101] PBCs of the P crystal cross the contact interface and "continue" in the [100] PBCs of the T individual, experiencing the same angular deflection (Figure 2). It is worth noting that the structural order of the strong Ca−SO_4 bonds is slightly modified by the transition occurring between the two kinds of PBC. The symmetry relating the water molecules is only perturbed in the interface layer. Therefore, the equilibrium structure of the 100 contact twin is fairly similar to that of the normal crystal, since only hydrogen bonds are quite distorted at the twin interface. Reasonably, this is the main reason why the 100 contact twin energy (γ_{PT}^{100}) acquires the very low value of 13.6 erg cm^{-2}.

5.2. The 001 Contact Twin. In Figure 3, the [010] projection of the 001 contact twin is shown. The difference with respect to the 100 interface is striking, because of the sharp discontinuity experienced by the PBCs across the twin interface:

- The [001] PBC of the P individual, which is made by the stacking of *iso*-oriented SO_4 tetrahedra, continues in the [101] PBC of the T individual, where the alternating tetrahedra are mutually related by a ≈90° rotation around the [010] axis. The reciprocal situation occurs for the [101] PBC of the P individual.
- The location of the water molecules within the d_{200} slice (parallel to both $[001]_P$ and $[010]_{P,T}$ directions) is markedly different with respect to those belonging to the $d_{20\bar{2}}$ slice (parallel to both $[101]_P$ and $[010]_{P,T}$ directions).

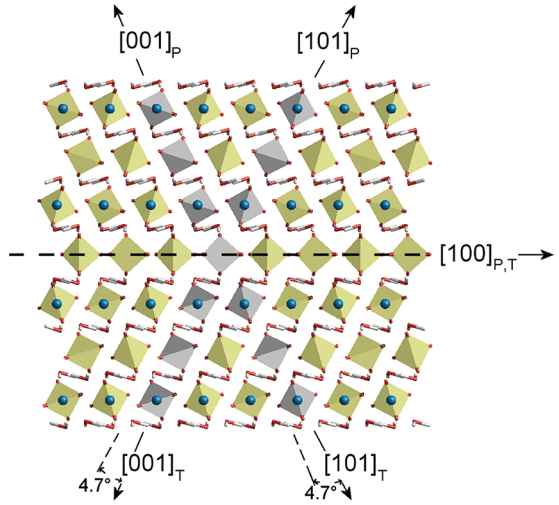

Figure 3. [010] projection of the 001 contact twin. A sharp discontinuity stands out in the orientation of tetrahedra within the ···SO_4−water−SO_4···sequence, when the [001] and [101] PBCs belonging to P individual cross the twin interface and continue in the T individual, as [101] and [001] PBCs, respectively. The deviation angle across the interface does not reach 5°.

Furthermore, there is an evident singular d_{002} layer, parallel to the twin interface, where the orientation of the groups SO_4 is intermediate between that in P and T individuals. In the bulk, the oxygen atoms linked to sulfur are arranged in four planes parallel to 001, while in the singular layer, marking the transition between the two crystals, the oxygen atoms are arranged on three planes: Indeed, two oxygens lie on the same plane marked by a dashed line in Figure 3.

In the singular layer, the distance between oxygen atoms in closer contact is 6.80 Å, while it is 4.46 Å in the two adjacent layers. In the bulk, the corresponding distances increase to 6.94 and 4.53 Å, respectively. As shown in Figure S6 in the Supporting Information, the variations of the longer O−O contacts occur over eight tetrahedral layers, indicating damped librations of the groups SO_4.

The librations are accompanied by oscillations of the distances between adjacent d_{002} atomic layers in direction perpendicular to the 001 interface, as shown in Figure S7 in the Supporting Information. From the figures, one sees that the layers of the water oxygens (O_W) move in phase with the calcium planes, while the sulfur planes are in antiphase with calcium. It is interesting to compare the amplitude of the interfacial deformation of the 100 twin with that of the 001 twin. Expressing the highest values of deformation as a percentage of the equidistance in the bulk, we obtain the following values:

(i) 001 twin: O_W, +3.1 and −1.6%; Ca, +2.5 and −1.2%.
(ii) 100 twin: O_W, +0.98 and −0.3%; Ca, +0.43 and 0%.

These amplitudes are, in some cases, even higher than those of the layers at the surface of the slab (e.g., Figure S7a in the Supporting Information), at variance with our finding in the

dx.doi.org/10.1021/cg201031s | Cryst. Growth Des. 2012, 12, 264−270

case of the twin 100. We observe only very small translations and oscillations of atoms in directions lying in the OCP. The 001 contact twin energy (γ_{PT}^{001} = 145 erg cm^{-2}) is an order of magnitude higher than that of the 100 twin.

5.3. The 10$\bar{1}$ Contact Twin. The [010] projection of the 10$\bar{1}$ contact twin is represented in Figure 4a. The discontinuity

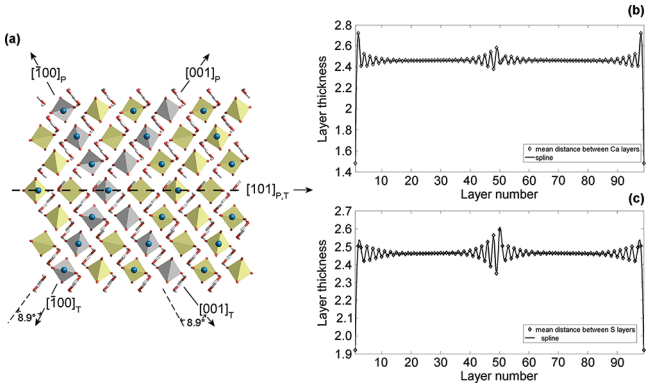

Figure 4. (a) [010] projection of the $\bar{1}$01 contact twin. The PBCs $[\bar{1}00]_P$ and $[001]_P$ cross the interface of the contact twin encountering a structural discontinuity analogous to that of the 001 twin law. The deviation angle across the interface increases, in this case, to ∼8.9°. The mean distances between the Ca (b) and the sulfate (c) layers are not symmetrically distributed around the $\bar{1}$01 twinned interface.

encountered by the PBCs [$\bar{1}$00] and [001] across the twin interface is strictly analogous to that just described for the 001 contact twin, as follows from the comparison between Figures 3 and 4a. At variance with the 001 contact twin, the angle of deviation of the PBCs across the interface does reach ∼8.9°. This clearly suggests that the transition from P to T individual should be even more expensive than that of 001 contact twin law.

Moreover, there is also in this case a singular $d_{20\bar{2}}$ layer, parallel to the twin interface, where the sulfate tetrahedra rotate to a position intermediate between those in the P and T crystals. The coordination of the two water molecules in the singular layer changes as well: one molecule follows the repeat sequence in the P crystal, while the other the sequence of water in the T crystal. Figure 4b,c shows the nonsymmetrical displacements of calcium and sulfur atoms close to the 10$\bar{1}$ twin interface.

Typically, the amplitude of the rotations of the SO_4 groups and H_2O molecules and the atomic translations at the interface between the two individual are high, and the transition from the P to the T structure involves the movements of all particles over several layers. Summing up, it is not surprising that the twin energy associated with the number of deeply perturbed layers on the two sides of the twin interface increases, in this case, to the value of 255 erg cm^{-2}.

5.4. The $\bar{2}$01 and the 101 Contact Twins. The last two contact twins will be treated together because of the common features of their twin interfaces. No trace remains, indeed, of the local symmetry that characterizes the 100 and 001 interfaces and, to a lesser extent, the $\bar{1}$01 contact twin. This can be clearly seen in Figure 5a,b, where the interface layers are expanded and organized in singular 2D structures different from the layers in the bulk.

Figure 5a,b shows the structure of the $\bar{2}$01 and 101 contact twins. One can notice the expansion of the interfacial regions in direction normal to the twin composition plane and the complex correlated rotations of the SO_4 tetrahedra and water molecules. All atoms experience translations parallel and perpendicular to the ideal $\bar{2}$01 plane, and consequently, the structural disorder extends, in the $\bar{2}$01 twin, over five layers of thickness $1/2d_{\bar{2}01}$. In the 101 twin, the SO_4 tetrahedra rotate to such an extent that a layer is formed where a plane of oxygen atoms is subparallel to 101. In this case, high angle rotations of the tetrahedra and of the water molecules occur over seven layers of thickness $1/2d_{101}$.

The number of PBCs crossing the interface is the same for both twins (i.e., PBCs [100], [001], and [101]), but the angular deflection experienced in the transition from the P to the T crystal is clearly larger in the 101 twin. In particular, the structural disorder and the lack of local symmetry at the interfacial level have a dramatic effect on the twin energy that practically increases of an order of magnitude with respect to γ_{PT}^{100}. As a matter of fact, $\gamma_{PT}^{\bar{2}01}$ = 826 and γ_{PT}^{101} = 848 erg cm^{-2}, respectively.

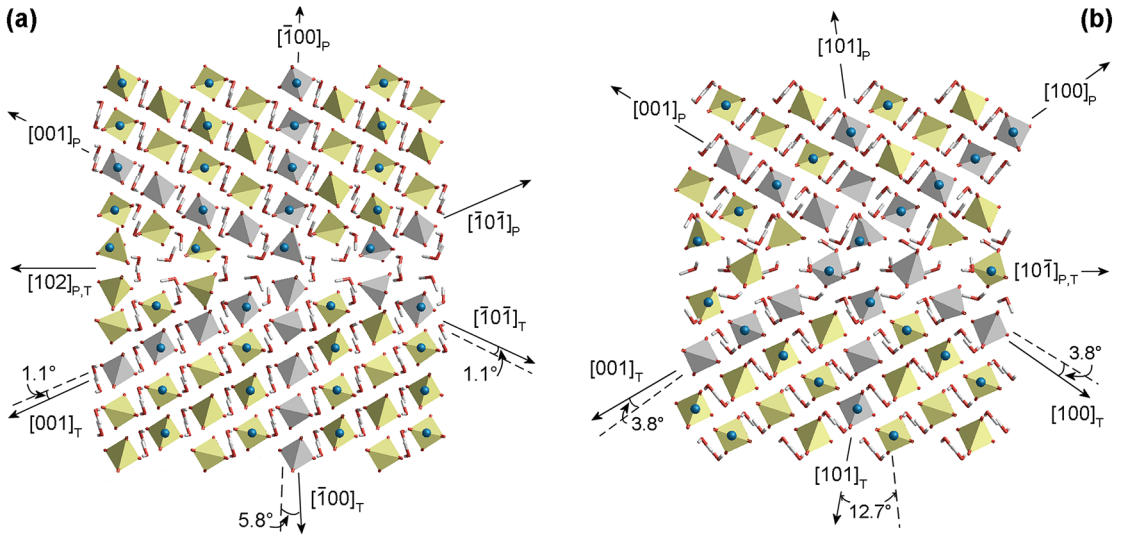

Figure 5. [010] projections of the (a) $\bar{2}$01 and (b) 101 contact twins.

dx.doi.org/10.1021/cg201031s | Cryst. Growth Des. 2012, 12, 264−270

6. CONCLUSIONS

The essential features of the five contact twins of gypsum are summarized in Table 3. For each geometrical law, the character of the OCP and the twin energy are indicated.

Table 3. Features of the Five Twin Laws of Gypsum[a]

twin law	character of the OCP	γ_{PT} (erg cm^{-2})
100	S	13.6
001	S	145
$10\bar{1}$	S	255
$\bar{2}01$	K	826
101	K	848

[a]Twin energy values (γ_{PT}) reflect the deep difference due to the character of the face on which the contact twin is supposed to form.

The five twins can be grouped in three classes, according to the magnitude of the twin energy: the 100 law, the couple 001 and $10\bar{1}$, and, finally, the couple made by the $\bar{2}01$ and 101 laws. Some comments further justify this classification.

(a) The 100 law can be assumed as the touchstone for the other laws. The 100 surface shares the S character with the 001 and $10\bar{1}$, but its twin energy is an order of magnitude lower. As the nucleation frequency of twins (either 2D or 3D) exponentially depends on the corresponding activation energy (which, in turn, is linearly related to the twin energy), the probability of formation of both 001 and $10\bar{1}$ contact twins should be by far lower than that of the 100. Many factors contribute to determine the peculiarity of the 100 contact law:
  (i) Among the {100}, {001}, and $\{10\bar{1}\}$ S forms, the {100} is the only one belonging to the [010] zone, which enters the athermal ES of the crystal, because of the low value of its specific surface energy.
  (ii) The 100 twin interface, among the five investigated, is the only one that is crossed by the [101] and [001] PBCs without change of the PBC structure.
  (iii) As a consequence, the {100} surfaces are the only ones where a 2D nucleation can occur both for normally oriented nuclei[4] and for twinned ones.

(b) The investigation on the 001 law deserves a novel feature: in spite of the usual tendency to neglect the 001 plane as a possible OCP, the formation of 001 contact twins seems to be favored with respect to the $10\bar{1}$ ones because the ratio $\gamma_{PT}^{\bar{1}01}/\gamma_{PT}^{001}$ is about 1.76.

This should not be surprising as the PBCs crossing both of the interfaces undergo the same structural change, but the angle of deviation at the $10\bar{1}$ interface is close to twice the value measured in the 001 twin. Such a difference reflects the slight asymmetry characterizing the $10\bar{1}$ contact interface when compared to the highly symmetrical 001 one (see Figure S7 in the Supporting Information and Figure 4b,c).

A second considerable finding is the difference ($\gamma_{PT}^{\bar{1}01} - \gamma_{PT}^{100}$) ≈ 131 erg cm^{-2}. This large value establishes, on a theoretical base, a hierarchy between two contact twin laws, and it accounts for the experimental results obtained by Kern and Rehn[21] who observed that the occurrence frequency of the 100 contact and penetration twins is more or less the same in growth from pure aqueous solution, while $10\bar{1}$ contact twins were never observed, under the same temperature and supersaturation conditions.

(c) The high twin energy of the remaining laws, that is, the $\bar{2}01$ and 101, can be understood referring to the Hartman's model of the growth twins.[22] As mentioned above, the $\bar{2}01$ and 101 interfaces differ from all of the preceding ones by the degree of structural disorder and by the sharp discontinuity of the structures of the PBCs when crossing the twin interfaces. Moreover, the $\bar{2}01$ and 101 twin energy increases with the angles of misalignment of the respective PBCs. This behavior is a consequence of the K character of the $\{\bar{2}01\}$ and {101}forms. In other words, a kinked (K) face, which is the best example of a crystal surface instability, does not have surface sites for the formation of 2D islands or 1D steps (either normally oriented or twinned). Then, the conditions necessary to the twin formation cannot be fulfilled by a K face, unless the adsorption of foreing substances determines either a K → S or a K → F transition.

Consequently, only $\bar{2}01$ and 101 penetration twins should be observed in growth from pure aqueous solution, since the water adsorption is not sufficient to reduce the surface energy by such an amount to allow the formation of contact twin possible. As a matter of fact, the adhesion energy ($\beta_{adh}^{solution}$) due to the solvent adsorption cannot exceed the value of $2\gamma_{water} \approx 150$ erg cm^{-2}, as it follows from Young's and Dupré's formulas.

Summing up, in this paper, we analyzed, in the light of the Hartman–Perdok theory, the twin geometry and the surface properties of the OCPs and found that the structural features correspond well to the relative stability of the contact twins obtained from their energy.

APPENDIX

The first study on the growth twins of gypsum is due to the Kern's School. A first experimental paper, dealing with the gypsum growth from pure aqueous solutions, is by Kern and Rehn.[21] The interpretation of the results on the growth twins was integrated by Simon,[15] who analyzed the mechanisms of formation of both contact and penetration twins. In these works, a reference was made to the morphological frame of Des Cloizeaux[23] that was used in two different versions:

(i) Kern and Rehn[21] adopted the original frame by Des Cloizeaux[23], which reads:

a: b: c = 0.68994: 1: 0.41241; β = 80°42′

according to Dana[24] and indexed the two main twin laws of gypsum as (100) and $(\bar{1}01)$.

(ii) Simon,[15] reversing the *z*-axis, used another frame:

a: b: c = 0.6910: 1: 0.4145; β = 98°52′

and indexed the main twin laws of gypsum as (100) and (101), respectively.

These two choices were synthesized by Simon[15] adopting the frame by De Jong and Bouman, which is related, within the limits of the experimental errors, to the frame by Gossner:[25]

$$a_0\ (\text{Å}) = 10.47;\ b_0\ (\text{Å}) = 15.15;\ c_0\ (\text{Å}) = 6.28;\ \beta = 98°52'$$

which is, in turn, coherent with the item (ii).

Hence, the relations between the indexes of the faces in the two reference frames: Des Cloizeaux (DC) and De Jong–Bouman (DJB)

dx.doi.org/10.1021/cg201031s | Cryst. Growth Des. 2012, 12, 264–270

depend on the relations between the vectors:

$$(\tau_1')_{DC} = (-2\tau_1 - \tau_3)_{DJB};\ (\tau_2')_{DC} = (-\tau_2)_{DJB};$$
$$(\tau_3')_{DC} = (\tau_3)_{DJB}$$

$$\{h'k'l'\}_{\text{Des Cloizeaux}} = \begin{pmatrix} -2 & 0 & -1 \\ 0 & -1 & 0 \\ 0 & 0 & 1 \end{pmatrix} \{hkl\}_{\text{De Jong–Bouman}}$$

Another way of indexing the most frequently occurring twins was adopted by A. M. Cody and R. D. Cody,[9,10,26,27] who referred to the morphological F cell of Dana.[24] Care must be taken in working with the morphologies described in their papers, since some ambiguities arise from the face indexing.

■ ASSOCIATED CONTENT

Supporting Information

The occurrence frequency of the five twin laws of gypsum; the character (in the sense of Hartman–Perdok) of the different surface profiles of the (100), ($\bar{1}$01), (001), (20$\bar{1}$), and (101) faces of gypsum; and the variations of the O–O distances and layer thickness as a function of the number of layers in the (001) twinned slab. This material is available free of charge via the Internet at http://pubs.acs.org.

■ AUTHOR INFORMATION

Corresponding Author

*Tel: +39 011 670 5127. Fax: +39 011 670 5128. E-mail: marco.rubbo@unito.it.

■ ACKNOWLEDGMENTS

We thank Prof. R. Kern for the fruitful discussions and two unknown reviewers for their helpful comments.

■ REFERENCES

(1) Massaro, F. R.; Rubbo, M.; Aquilano, D. *Cryst. Growth Des.* **2010**, *10*, 2870–2878.
(2) García-Ruiz, J. M.; Villasuso, R.; Ayora, C.; Canals, A.; Otálora, F. *Geology* **2007**, *35*, 327–330.
(3) Massaro, F. R.; Rubbo, M.; Aquilano, D. *Cryst. Growth Des.* **2011**, *11*, 1607–1614.
(4) Rubbo, M.; Bruno, M.; Aquilano, D. *Cryst. Growth Des.* **2011**, *11*, 2351–2357.
(5) Follner, S.; Wolter, A.; Helming, K.; Silber, C.; Bartels, H.; Follner, H. *Cryst. Res. Technol.* **2002**, *37*, 207–218.
(6) Mallard, E. *Traité de Cristallographie Géométrique et Physique*; Dunod: Paris, France, 1879.
(7) Friedel, G. *Leçons de Cristallographie*; Berger-Levraut: Paris, France, 1926.
(8) Curien, H.; Kern, R. *Bull. Soc. Franç. Minér. Crist.* **1957**, *80*, 111–1321.
(9) Cody, A. M.; Cody, R. D. *J. Cryst. Growth* **1989**, *98*, 721–730.
(10) Cody, A. M.; Cody, R. D. *J. Cryst. Growth* **1989**, *98*, 731–738.
(11) De Jong, W. F.; Bouman, J. *Z. Kristallogr.* **1938**, *100*, 275–276.
(12) Cole, W. E.; Lancucki, C. J. *Acta Crystallogr.* **1974**, *B30*, 921–929.
(13) Hartman, P.; Heijnen, W. M. M. *J. Cryst. Growth* **1983**, *63*, 261–264.
(14) Friedel, G. *Bull. Soc. Franç. Min. Cristal.* **1912**, *35*, 45–49.
(15) Simon, B. *Contribution à l'étude de la Formation des Macles de Croissance*; Thèse docteur ès-sciences physiques: Marseille, France, 1968.
(16) Aquilano, D.; Boistelle, R. *Acta Crystallogr. A* **1977**, *33*, 642–648.
(17) Hartman, P. In *Crystal Growth: An Introduction*; Hartman, P., Ed.; North Holland Publishing Co.: Amsterdam, 1973; pp 367–402.
(18) Fleming, S.; Rohl, A. *Z. Kristallogr.* **2005**, *220*, 580–584.
(19) Gale, J. D. *Faraday Trans.* **1997**, *93*, 629–637.
(20) Adam, C. D. J. *Solid State Chem.* **2003**, *174*, 141–151.
(21) Kern, R.; Rehn, B. *C. R. Acad. Sci. Paris* **1960**, *251*, 1300–1302.
(22) Hartman, P. *Z. Kristallogr.* **1956**, *107*, 225–237.
(23) Des Cloizeaux, A. L. O. L. *Bull. Soc. Franç. Min.* **1886**, *9*, 175.
(24) Dana, E. S. *The System of Mineralogy*, 6th ed.; Wiley: New York, 1892.
(25) Gossner, B. *Z. Kristallogr.* **1937**, *96*, 488.
(26) Cody, R. D.; Cody, A. M. *Cryst. Res. Technol.* **1988**, *23*, 1437–1441.
(27) Cody, A. M.; Cody, R. D. *J. Cryst. Growth* **1991**, *113*, 508–519.